DESIGN AND TEST OF A BREADBOARD INTERPLANETARY LASER TRANSPONDER

John Degnan, Jan McGarry, Phillip Dabney,
Thomas Zagwodzki, Michael Tierney, and Matthew Weatherly
Geoscience Technology Office, Code 920.3
NASA Goddard Space Flight Center
Greenbelt, MD 20771 USA

ABSTRACT

At the last SLR Workshop in Shanghai, the feasibility of an asynchronous (i.e. independently firing) interplanetary laser transponder, capable of ranging between Earth and Mars and using the automated SLR2000 system as an Earth base station, was suggested. Since that time, we have received a small amount of discretionary funding to further explore the transponder concept and to develop and test an engineering breadboard. Candidate operational scenarios for acquiring and tracking the opposite laser terminal over interplanetary distances have been developed, and breadboard engineering parameters were chosen to reflect the requirements of an Earth-Mars link. Laboratory tests have been devised to simulate the Earth-Mars link between two independent SLR2000 transceivers and to demonstrate the transfer of range and time in single photon mode. The present paper reviews the transponder breadboard design, an operational scenario recently developed for an asteroid rendezvous, and the laboratory test setup.

The optical head of the transponder breadboard fits within a cylinder roughly 15 cm in diameter and 32 cm in length and is mounted in a commercial two axis gimbal driven by two computer-controlled stepper motors which allows the receiver optical axis to be centered on a simulated Earth image. The optical head is built around a small optical bench which supports a 14.7 cm diameter refractive telescope, a prototype 2 kHz SLR2000 microlaser transmitter, a quadrant microchannel plate photomultiplier (MCP/PMT), a CCD array camera, spatial and spectral filters, assorted lenses and mirrors, and protective covers and sun shields. The microlaser is end-pumped by a fiber-coupled diode laser array. An annular mirror is employed as a passive transmit/receive (T/R) switch in an aperture-sharing arrangement wherein the transmitted beam passes through the central hole and illuminates only the central 2.5 cm of the common telescope (adequate to achieve a 10 arcsecond full laser beam divergence) while the receiver uses the remainder of the 14.7 cm aperture. Additional electronic instrumentation includes the diode pump array and associated heat sink and current drivers, rubidium frequency standard, timing distribution module, range gate generator, correlation range receiver, and system computer.

Acquisition of the opposite transponder terminal requires a search within a three-dimensional volume determined by the initial pointing uncertainty and a maximum 500 microsecond uncertainty in the laser time of fire at the opposite terminal for totally uncorrelated Earth and spacecraft clocks. The angular search is aided by a sensitive CCD array capable of imaging the Earth, Moon, and surrounding stars within the nominal $\pm$ 0.5 degree cone of uncertainty associated with the initial pointing of a spacecraft body or microwave communications dish. Using the independent two axis gimbal, the system computer centers and holds the Earth image in the array ensuring that a properly directed beam from Earth is detected in the receiver. Using the Moon and/or a greatly abridged star catalog and knowledge of the planetary ephemerides, the system controller computes the direction and magnitude of the differential point-ahead/look-behind angle in the instrument coordinate system (on the order of an arcminute or less) and independently drives a pair of Risley prisms to offset the laser transmitter from the receiver optical axis. The search in the third dimension, range, is carried out by using a priori information on range rate and laser jitter and by breaking up the 500 microsecond interval between laser fires into appropriately sized time bins to help isolate the signal using post-detection Poisson filtering techniques. Once acquired, the quadrant detector and correlation range receiver can further improve the accuracy of the pointing and time lock. The same instrument can be used to map the surface topography of a planet, moon, asteroid, or comet from orbit at kHz rates.

1. INTRODUCTION

Transponders fall into two basic classes, i.e. *echo* and *asynchronous*. The type typically used in underwater acoustic sounders or microwave aircraft transponders is the *echo transponder* in which a pulse emitted from terminal „A“ is detected by terminal „B“ which then generates a response pulse subsequently detected by „A“. The delay between the received and transmitted pulse at a given terminal, which is usually either known a priori through careful calibration or controlled via active electronics, is subtracted from the observed roundtrip time before computing the target range. Alternatively, the delay can be measured locally and transmitted to the opposite terminal via a communications link. In an *asynchronous transponder*, the two terminals independently fire pulses at each other at a known repetition rate. Terminal „A“ records the times of departure of its own transmitted pulses and the (intermittent) times of arrival of pulses from „B“ and vice versa. The departure and arrival times measured at each terminal are then communicated to, and properly paired at, a common processor which then calculates a range and clock offset for the two terminals [1]. As we will discuss later, knowledge of the repetition rate at the opposite terminal helps us distinguish signal photons from background counts in much the same way that a „lock-in amplifier“ extracts a very low level, but coherent, signal from random background noise.

At the last SLR Workshop in Shanghai, the feasibility of an asynchronous interplanetary laser transponder, capable of ranging between Earth and Mars, using NASA’s automated SLR2000 system [2] as an Earth base station, was suggested. It was demonstrated through analysis that a compact asynchronous microlaser transponder, using a 15 cm collecting aperture, each operating at 2 kHz rates between Mars and Earth, is potentially capable of generating up to several thousand two way measurements per minute and several tens of thousands of one way measurements per minute using low power (300 mW @ 532 nm), passively Q-switched, Nd:YAG microlaser transmitters at each terminal [1]. It was also shown that two way measurements allow precise determination of the intersystem range and the clock offset between the Earth and remote terminals whereas rapidly occurring one way ranges help to acquire and maintain a common boresight with the opposite terminal. Due to long one way interplanetary light travel times extending up to 30 minutes (e.g., from Earth to the asteroid belt on the far side of the Sun), the absolute accuracy of the range and clock offset measurements is determined more by the frequency accuracy and stability of the groundbased and spaceborne clocks than by errors in the range vernier or propagation delays in the transmission channel, which can be reduced to the subcentimeter level as in SLR. Decimeter accuracy interplanetary range measurements and subnanosecond time transfer would appear to be readily achievable with conventional space-qualified atomic clocks [1]. However, if a ground-based maser were used to govern the SLR2000 timing and to monitor the phase variations of the onboard atomic clock via the time transfer process, significantly greater accuracies at the centimeter, or even subcentimeter, level might be achievable [1]. Based on past experience with the Viking lander on Mars, current microwave system *precision* appears to be limited at the few meter level [3]. Furthermore, unlike microwaves, the absolute *accuracy* of an optical link is not affected by uncertainties in propagation delays induced by the interplanetary solar plasma.

Since the last Workshop, we have received a small amount of funding from the Goddard Director’s Discretionary Fund (DDF) to further explore the transponder concept and to develop and test an engineering breadboard. The breadboard engineering parameters were chosen to reflect the requirements of an Earth-Mars laser transponder link. Laboratory tests have been devised to simulate the Earth-Mars link between two independent SLR2000 transceivers and to demonstrate the transfer of range and time in a photon counting mode. Candidate operational scenarios for acquiring and tracking the opposite laser terminal over interplanetary distances were developed. We also had an independent opportunity to develop a concept for an asteroid rendezvous mission which combines transponder and altimetry functions in the same instrument. The present paper further develops the transponder concept outlined in [1], describes an operational scenario for terminal acquisition and tracking, and reviews the transponder breadboard design and the laboratory test setup.

2. MAXIMIZING THE SIGNAL DETECTION RATE VIA SINGLE PHOTON DETECTION

In this section, we will demonstrate that, for a given average laser power and aperture, the maximum signal detection rate is achieved through the use of single photon detection and low energy, high repetition rate lasers. The mean number of signal photoelectrons recorded by the receiver on a single laser fire is given by the equation

$$n_s = \frac{C_X EA}{R^{N_X}} \qquad (1)$$

where E_A is the pulse energy transmitted from terminal „A“ , A_B is the area of the receiving telescope at terminal „B“, R is the distance between the two terminals, and C_{AB} is a *transponder constant* given by

$$C_T = \frac{4\eta_q \eta_t \eta_r T_a T_{a'}}{h\nu\theta_t^2 (4\pi)} \qquad (2)$$

and η_q is the detector quantum efficiency, $h\nu$ is the laser photon energy, T_A and T_B the one-way atmospheric transmissions at Terminal „A“ and „B“ respectively (appropriate for two terminals on planetary surfaces), Ω_t is the laser transmitter solid angle, and η_t and η_r are the optical throughput efficiencies of the transmitter and receiver optics respectively. The mean signal at the opposite terminal is obtained by simply interchanging A and B in the above equations.

We can choose to write (1) in terms of the average laser power, i.e.

$$n_s = \frac{C_X PA}{f_{QS} R^{N_X}} \qquad (3)$$

where f_{QS} is the Q-switching frequency (laser repetition rate) in Hz which we will assume to be common to both terminals.

Now, the mean number of range returns per second recorded at either terminal is given by the product of the laser fire rate and the probability of detection for that terminal, i.e.

$$f_R = f_{QS} P_D(n_s, n_t) = f_{\max} \frac{1}{n_s}\left(1 - e^{-n_s} \sum_{k=0}^{n_t - 1} \frac{n_s^k}{k!}\right) \qquad (4)$$

where we have solved for f_{QS} in (3). The probability of detection in the low signal limit is given by Poisson statistics and depends on both the mean signal strength, n_s, and the detection threshold, n_t. Thus, for terminal „B“, the maximum signal detection rate is

$$f_{\max}^B = \frac{C_{AB} P_A A_B}{R^2} \qquad (5)$$

where we refer to P_AA_B as the *Mixed Power-Aperture Product* to reflect the fact that it contains properties of two different terminals. In Figure 1, we plot the normalized detection rate, N / N_{max}^{X} and demonstrate that the parameter N_{max}^{X} corresponds to the maximum detection rate in the limit of small mean signal strength and single photoelectron detection. We draw the following conclusions from the figure:

> For a given Mixed Power-Aperture Product, the maximum rate of transponder signal detection is obtained by using single photon detection and a high repetition rate laser with low energy per pulse such that the mean signal count received per laser fire is n_s<<1.
>
> For higher detection thresholds, the frequency of signal returns peaks at a value lower than f_{max} for mean signal counts near the threshold value (e.g. at n_s = 1.8 pe for n_t = 2 pe and at n_s = 3.3 pe for n_t = 3 pe, etc.). To achieve comparable return rates at thresholds higher than one photoelectron, the average laser power would have to be increased significantly (e.g. by factors of 3.4 and 5.1 for thresholds of 2 and 3 pe respectively).

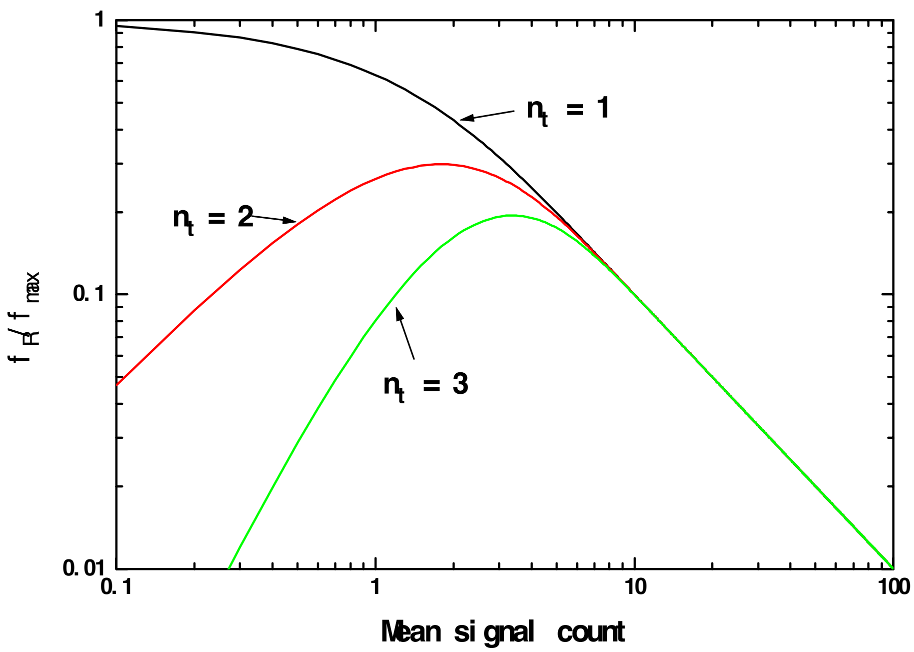

Figure 1: Normalized rate of detection as a function of the detection threshold, n_t, and the mean signal count, n_s.

Now, from (3), the ratio of the mean signal strengths at the two terminals is given by

$$\frac{n_s^B}{n_s^A} = \frac{C_{AB}}{C_{BA}} \frac{P_A A_B}{P_B A_A} \cong \frac{P_A}{A_A} \frac{A_B}{P_B} \qquad (6)$$

where, from (2), the approximation holds if the laser beam divergence and detector and optical throughput efficiencies are roughly equal at both ends of the link $(C_{AB} \cong C_{BA})$. Furthermore, the above ratio is approximately unity if the *Power-to-Aperture Ratio* is the same at both ends of the transponder link; i.e. $P_A/A_A = P_B/A_B$. We will refer to this as a *balanced* system. Note that the signal detection rate is proportional to the *Mixed Power-Aperture*

Product, $P_A A_B$, and that, for a balanced system, $f_{\max}^{B} \approx f_{\max}^{A}$. Thus, we can increase the power and aperture at the Earth station proportionally to maintain the same Power-to- Aperture ratio while simultaneously reducing the transponder laser power and receive aperture by the same factor in order to conserve limited spacecraft resources while still maintaining the same signal detection rate at both terminals.

3. SOURCES OF NOISE

While Figure 1 provides us with some interesting conclusions, real photon counting transponders must contend with a noise background. The radiative output of the Earth and other celestial objects (e.g. background stars) within both the receiver spatial field-of-view (FOV) and spectral bandpass are generally small, but inescapable, sources of noise as is the dark count rate in the detector. Dark count rates tend to be relatively low (several thousand counts per second) in the visible MicroChannel Plate PhotoMultiplier Tubes (MCP/PMT's) typically used in laser ranging and somewhat higher in visible Avalanche Photodiodes (APD's) (which also have higher quantum efficiencies). Direct solar illumination of the transponder optics and the resulting internal scatter is another potential source of background noise. System baffling and stray light rejection can be important considerations since, at the asteroid belt for example, the Sun is never more than about 25 degrees away from the transponder line-of-sight to Earth. Thus, if the spacecraft transponder is operating in one of the following scenarios - interplanetary cruise phase, in orbit about a planet or moon, or on the surface of an airless moon or asteroid - the noise background count rate can be made relatively low through careful filtering and stray light control.

In the more extreme case of a planetary lander operating in local daylight conditions, scattered sunlight from the local atmosphere and/or clouds is the dominant source of noise. This is analogous to the photon-counting SLR2000 system operating in daylight, and similar detection techniques must be applied. Additional receiver interference from outgoing laser radiation backscattered from the planetary atmosphere can largely be suppressed in the transponder by designing it to be bistatic (truly separate transmit/receive optics) or by otherwise spatially isolating the transmit/receive beams (e.g. „aperture sharing“). A one to two inch transmit aperture is more than sufficient to generate a highly collimated 10 arcsecond beam given the TEM_{00} spatial quality of the microlaser. In SLR2000, absolute eye safety requirements, coupled with overall tracking mount size and cost considerations, did not permit spatial separation of the transmit and receive beams.

In general, various types of filters are employed to reduce the background noise in active laser rangers. Specifically, one can limit the spectral width of the bandpass filter (*spectral filtering*), reduce the receiver field-of-view to the minimum value which encompasses the transmit beam divergence and its potential pointing variations and/or coalignment errors with the receiver (*spatial filtering*), gate the receiver so that only photons within a given time window about the expected signal return are accepted (*temporal filtering*), and raise the detection threshold to a value which largely eliminates the instrumental detection of false alarms (*amplitude filtering*). In photon counting systems, amplitude filtering cannot be used except in a statistical sense over many laser fires and must therefore be replaced by *post-detection Poisson filtering* as in SLR2000 [2,4]. This latter filter is crucial to photon-counting transponders on a planetary lander where, because of solar atmospheric scattering, the mean number of noise photoelectrons generated per laser fire can greatly exceed the mean number of signal photoelectrons per fire (usually less than one).

4. INITIAL ACQUISITION OF THE EARTH STATION IN ANGULAR SPACE

In developing the scenario for a laser transponder mission within the inner Solar System, we assumed that NASA's new photon counting SLR2000 system [2], or minor modification thereof, would serve as the Earth station. Besides achieving the highest measurement rate between the two terminals as described in Section 2, this approach allows us to take advantage of a likely future ground network and many of the new technology components which have been developed in support of it. These include the microlaser transmitter, quadrant detector, and correlation range receiver and software. The SLR2000 system operates at a repetition rate of 2 kHz, which implies a 500 μsec interval between laser fires. For simplicity, we will assume that the transponder uses similar components and operates at the same rate. A block diagram of a combined Microlaser Altimeter Transponder (MAT) instrument, recently proposed for a NASA Discovery mission to the asteroid Vesta, is shown in Figure 2. In altimetry mode, the instrument maps the asteroid surface from orbit and, in transponder mode, it provides precise range measurements and spacecraft clock offsets relative to the Earth station.

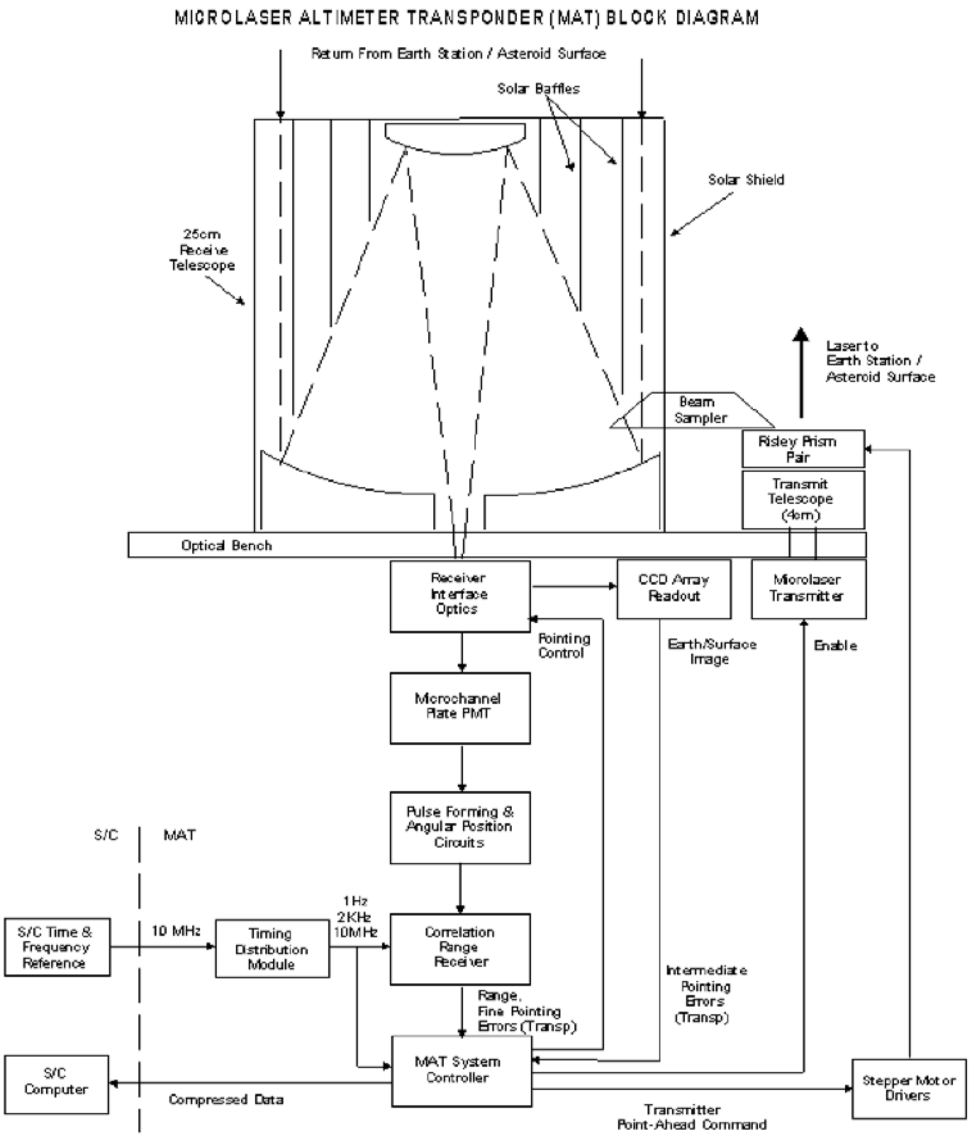

Figure 2: Block diagram of a combined Microlaser Altimeter Transponder (MAT) instrument proposed for a NASA Discovery Mission to the asteroid Vesta.

Acquisition of the opposite transponder terminal requires an initial search within a three-dimensional volume bounded by the initial angular pointing uncertainty and, for totally uncorrelated Earth and spacecraft clocks, a maximum 500 μsec uncertainty in the laser time of fire at the opposite terminal. The angular search for the opposite terminal is aided by a sensitive CCD array capable of imaging the Earth, Moon, and nearby stars within a nominal ± 0.5 degree cone of uncertainty. For a transponder mounted to the spacecraft body, this level of angular uncertainty is representative of the error associated with the pointing of a spacecraft during interplanetary cruise phase. It is also representative of the expected angular error in the case where the transponder is assumed mounted to a meter-class K-band microwave communications dish communicating with Earth. Using an independent two-axis transponder gimbal mount of limited angular range, the onboard computer can center and hold the Earth image in the CCD array. Space- qualified, high sensitivity CCD cameras with up to 2048 x 2048 pixel resolution are readily available yielding 4 μrad single pixel resolutions for a nominal 1°x1° array FOV. Since the full Earth disk subtends an angular width between 34 and 163 μrad (8 to 41 pixels across) from Mars at its farthest and closest points from Earth respectively, the center of the Earth image can be well resolved. Even when the Earth's „nightside" is largely directed toward the transponder, there is sufficient forward scattering of solar light by the Earth's atmospheric rim for detection [5].

Once the Earth is centered in the receiver FOV, receipt of laser pulses from Earth is ensured provided the Earth ground station pointing error is less than the ground laser beam divergence (nominally 50 μrad) and there is adequate signal. Angular errors due to uncertainties in planetary and most other ephemerides to important bodies in the inner Solar System are far smaller than the proposed beam divergence as are the pointing control errors in a well calibrated telescope. Furthermore, arriving photons will be detected by the quadrant ranging detector since the latter is co-aligned with the CCD array. As in SLR2000 [2], this permits fine pointing corrections of the transponder receiver at the subarcsecond level.

.

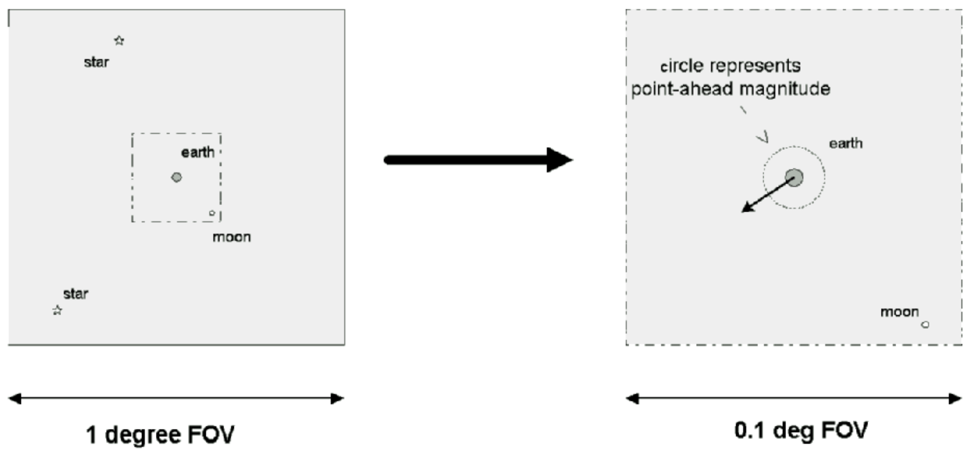

Figure 3: Simulated CCD camera display showing the centered Earth, Moon, and background stars used in the computation of the transmitter point ahead angle and direction. The circle around the Earth represents the magnitude of the angular offset as computed from the planetary ephemerides, and the arrow represents the Earth's forward motion as determined by other celestial objects (Moon, stars) in the camera FOV. The intersection of these two curves indicates the desired laser beam pointing.

5. TRANSMITTER POINT-AHEAD

In a general transponder experiment, the CCD Earth image tells us where the Earth was situated one transit time earlier whereas the narrow beam transmitter must be pointed to where the Earth will be one transit time later. In the more specific case of a Mars lander, an onboard knowledge of the approximate locations of the Earth and Mars in their respective solar orbits and planetary spin axis orientation and rotation rates allows a reasonably precise estimate of both the time of flight (TOF) and the differential pointing angle between the transmit and receive beams. Thus, one transit time later and in the image plane of our receiver CCD, the Earth will lie somewhere on the perimeter of a circle centered on our Earth image and having an angular radius equal to the differential pointing angle. The projection of the Earth's forward velocity vector in the receiver plane is needed to determine the precise point on the circle to which the laser beam should be directed. This can be inferred from simultaneous CCD observations of the Moon (although several magnitudes fainter than Earth) and/or star field within the camera FOV. The Moon is expected to be visible about 80% of the time [5] and, when it is not, background stars within the nominal 1° x 1° CCD FOV can be substituted as available. For a lander with known orientation relative to Earth, this angular uncertainty is greatly reduced.

Differential pointing of the transmitter can be most easily accomplished with a pair of azimuthally driven Risley prisms; the magnitude of the angular offset is determined by their relative position (which remains constant during a transponder experiment) and the direction is changed by driving them together to locate the precise point on the circle. Feedback to the receiver can be provided by a prism or two mirror reflector which samples the beam as it exits the transmit telescope and reflects it into the receiver for time logging and verification of the transmit angle.

6. ACQUISITION AND TRACKING OF THE EARTH STATION IN RANGE SPACE

Photon counting systems are governed by the laws of Poisson statistics. Post-detection Poisson Filters (PPF's) take advantage of the fact that the so-called „generating functions" for noise and signal are quite different. For example, in a satellite laser ranging (SLR) or interplanetary transponder system, the signal distribution is expected to be highly peaked in range space after one has applied appropriate corrections to the time-of-flight (TOF) measurements based on fairly good a priori knowledge of the range and range rate between the station and the target and the high precision of the range measurement itself. For the SLR example, if our a priori range and range rate corrections and satellite force models were perfect and additionally there were no range or time biases in the computed orbit, the corresponding „Observed Minus Calculated" (O-C) curve would place all of the signal photons within a thin horizontal strip centered in the range gate. In this highly idealized example, the temporal width of the signal data distribution within this strip would be determined by the timing precision of the range receiver and small atmosphere-induced fluctuations which, in modern SLR systems, is characterized by a one sigma RMS single-shot range scatter of about one cm [6]. In two-way transponders, the range-rate may not be known with the same precision, and there is additional uncertainty with respect to the precise time of fire at the other terminal due to the initial asynchronization of the ground and spaceborne clocks and laser fire jitter (which is measured directly in a single-ended ranging system). In real systems, range biases displace the signal from the center of the range window, and time biases or range rate errors introduce a slope in the signal data as in Figure 4a. Nevertheless, the signal data (indicated by black squares) will still be highly confined in range-space for appropriately short time intervals (called. a *frame*). Noise photons and detector dark counts (open squares), on the other hand, are randomly distributed throughout the entire range gate. Thus, one can subdivide the range window into smaller *range bins*, one of which has a high probability of collecting all of the signal photoelectrons received in the sequence of laser fires defining the frame. We refer to the 2D areas defined by the horizontal borders of the „range bins" and the vertical borders of the „frames" as *cells*. A consecutive sequence of frames is a *super-frame*. As in Figure 4b, a highly peaked histogram results when we have tested for and applied the optimum range-rate correction to the raw range data within a frame or super-frame. Thus, the search in the third dimension, range, is carried out by (1) breaking up the 500 μsec interval between the asynchronous laser fires into appropriately sized time bins to help isolate the signal; (2) applying corrections to the raw data using a priori information on range rate and laser jitter; and (3) applying a software filter to obtain and correct for any residual range-rate error.

We tentatively identify potential *signal cells* within a given frame by counting all of the photoelectrons generated within each cell and comparing it to a *frame threshold*. It is important that the frame threshold be chosen sufficiently high so that the probability of falsely identifying noise counts as signal in any given cell is appropriately low. On the other hand, the threshold must be sufficiently low so that one does not, with high probability, inadvertently dismiss the signal as noise. In Figure 4b, the ideal threshold would lie approximately midway between the histogram peak and the noise „floor". However, because of the potentially large number of cells in a frame (especially during target acquisition when range uncertainties are largest), a modest number of noise cells in a given frame can be falsely identified as signal even when the probability of false alarm for any given cell is relatively small.

This „balancing act" for threshold is not as difficult or stringent as it first seems since a powerful second test can be applied, if necessary, by requiring that cells in adjoining frames be „correlated". In the most general sense, this simply means that cells tentatively identified as containing „signal" in adjacent frames must obey applicable physical laws or constraints. For example, the physical laws governing satellite or spacecraft motion do not allow a satellite to make unexpected discontinuous jumps into widely separated range bins between frames. Thus, we can define a „valid trajectory“ as one where the satellite or spacecraft position changes by no more than one range bin in moving between frames and monotonically moves in the correct direction on either side of the Point of Closest Approach (PCA). This correlation requirement allows us, if necessary, to apply an additional and powerful „N of M“ test on multiple cells which survive the initial threshold test within each frame. For signal verification, the „N of M“ test requires that at least N cells, all satisfying the threshold criteria and lying on a valid trajectory, be detected within M frames (comprising a super-frame). Based on successful application of this test, any signal data in the up to (M-N) signal cells, which may have originally failed to meet the threshold criteria, can be successfully restored through interpolation between frames.

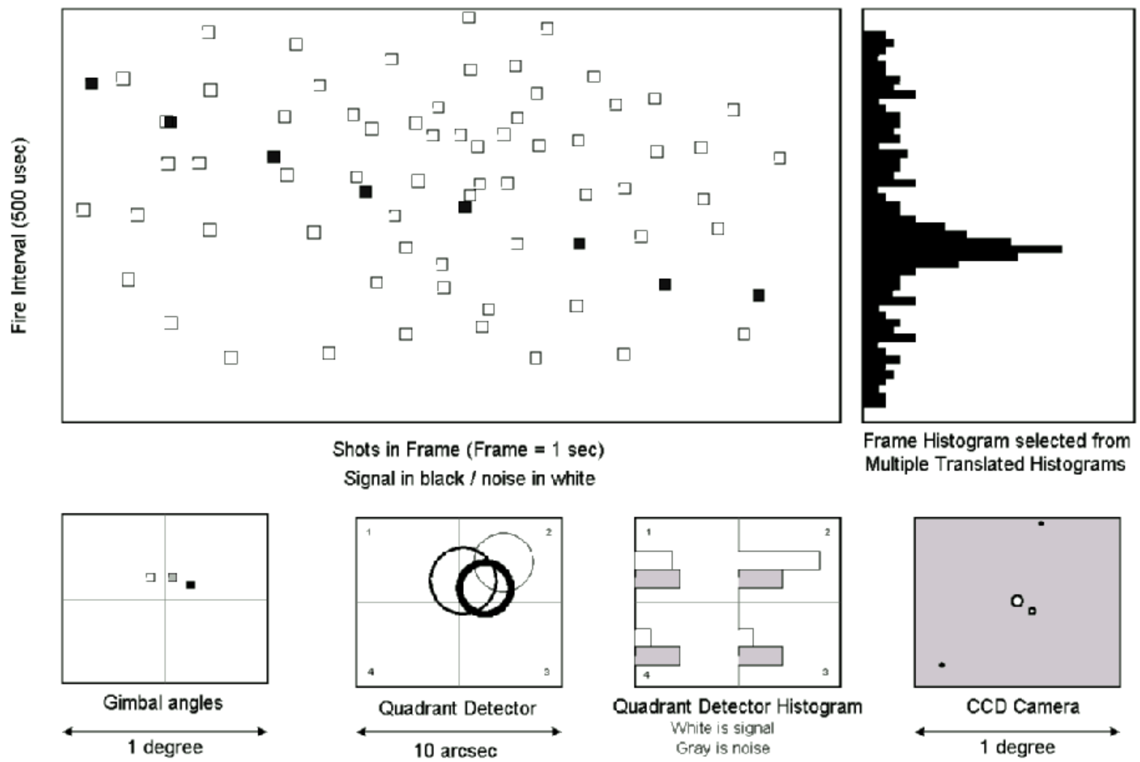

Figure 4: Breadboard transponder computer screen display. Clockwise from top: (a) a display of raw signal returns (black squares) modulo 500 microseconds (laser fire interval) against the noise background (white squares); (b) the maximum height range histogram generated after an optimum range rate correction has been selected to remove the slope; (c) a CCD display showing the Earth, Moon, and background stars; (d) signal and residual noise counts observed by the quadrant detector after the CRR removes the vast majority of noise counts residing in non-signal bins; (e) progress of pointing correction based on quadrant output for three successive frames (light to dark circles); and (f) the corresponding two-axis gimbal angle movements.

7. TRANSPONDER BREADBOARD DESIGN

The optical head of the transponder breadboard, shown in Figure 5, fits within a cylinder roughly 15 cm in diameter and 32 cm in length. It is sized for an Earth-Mars link. The optical head is built around a small aluminum optical bench designed to support a 14.7 cm diameter refractive telescope receiver, a prototype in-house 2 kHz SLR2000 microlaser transmitter, a quadrant microchannel plate photomultiplier (MCP/PMT), an Electrim Model EDC-1000M 324x242 pixel CCD array camera, spatial and spectral filters, assorted beam expanders, field lenses, relay mirrors, and protective covers and sun shields. The Nd:YAG microlaser (~9.5 mm diameter x 2.5 mm thick) is passively Q-switched by a thin disk (~9.5 mm diameter x 1mm thick) of Chromium-doped Yttrium Aluminum Garnet (YAG) and end-pumped by a commercial fiber-coupled diode laser array producing up to 10 Watts of CW power at the Nd:YAG pump wavelength of 808 nm. In lab experiments, where the signal levels at the receivers must be severely attenuated to achieve photon counting conditions, a low power ultrashort pulse laser diode modified to operate at 2 kHz (shown in the photo) has been employed in place of the microlaser. For ease of alignment, the laser is mounted on a New Focus Model 9801 5-axis Positioner. The quadrant detector in the photo is a Hamamatsu Model R5900U, but the faster SLR2000 Photek quadrant MCP/PMT can also be inserted. An annular mirror is employed as a passive transmit/receive (T/R) switch in an aperture-sharing arrangement wherein the transmitted beam passes through the central hole and illuminates only the central 2.5 cm of the common telescope (adequate to achieve a 10 arcsecond full laser beam divergence with the quasi-TEM_{00} laser output) while the receiver uses the outer annulus of the 14.7 cm aperture. The optical head is mounted in a commercial two axis gimbal driven by two computer-controlled stepper motors (Newport Research Corporation Model SL15A.VP) which allows the receiver optical axis to be centered on a simulated Earth image and/or signal source in response to intermediate and fine pointing corrections generated by the CCD array and/or quadrant detector respectively.

Additional electronic instrumentation not shown in Figure 5 includes the Optopower Inc. Model OPC-D010-808-HBHS/250 diode pump array and associated heat sink and current drivers, a Ball/Efratom Model FRK-L mil-spec rubidium oscillator, an in-house timing distribution module, in-house range gate generator, in-house correlation range receiver, and system PC.

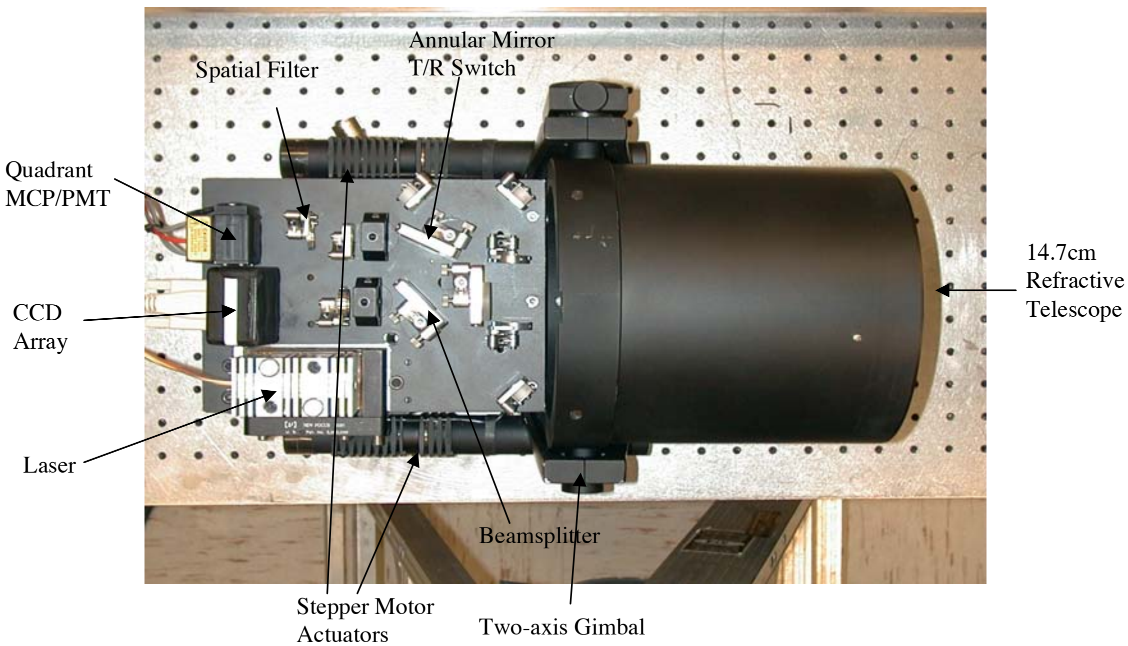

Figure 5: Top view of the Laser Transponder Breadboard.

8. TRANSPONDER TEST CONFIGURATION

The Interplanetary Laser Transponder Breadboard is installed on an optical bench in the same laboratory where the prototype SLR2000 correlation range receivers (CRR) are being tested. A block diagram of the transponder test setup is shown in Figure 6. To date, only a subset of the laboratory experiments have been conducted, but we hope to complete the remainder in the coming year.

Two versions of the SLR2000 CRR are currently available to us in setting up the two way link – the SLR2000 baseline configuration made up of rack-mounted commercial nuclear timing components (4 mm single shot limiting range resolution) and an enhanced version (1mm limiting resolution) based on the MLRO event timer [7]. In addition, we are developing a lower resolution (few cm) but very compact, all-digital event timer specifically for the altimeter/transponder application where the higher range resolution is not needed or justified. In transponder mode, the accuracy of the range measurement is expected to be limited, at least initially, at the decimeter level by the accuracy and stability of the onboard atomic clock [1]. In altimetry mode, spacecraft attitude knowledge is the limiting error source in measuring the distance to the underlying terrain.

.

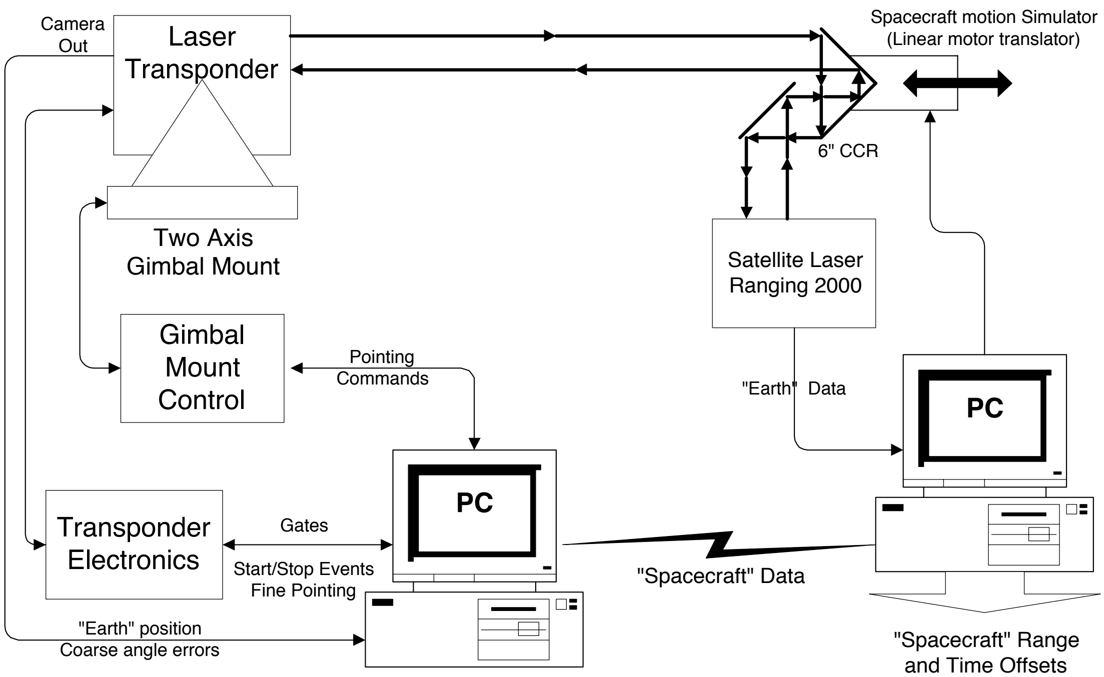

Figure 6: Transponder laboratory test setup at the Goddard Space Flight Center.

Each of the terminals independently fires a laser pulse at the other and detects the pulse from the other terminal in its receiver. The pulses are highly attenuated so that single photons are detected at the other end at a rate simulating the expected Earth-Mars link [1]. A computer-controlled moving corner cube common to both laser beams simulates an uncorrected range-rate error in the spacecraft motion. The receivers are driven by two independently controlled and uncorrelated rubidium frequency standards in order to test the time transfer capabilities of the transponder link.

Controlled white light sources in the FOV of each receiver allow the noise background to be varied over a wide range to simulate a variety of operational noise scenarios, i.e. from transponder in cruise phase to planetary lander.

Each terminal independently records its own fire times and detector events. The „spacecraft data“ is then ported to the „ground computer“ for final analysis of range and clock offset. The CCD and quadrant ranging detector provide intermediate and fine pointing error signals to keep the transponder optical axis centered on the opposite terminal.

9. COMBINED MICROLASER ALTIMETER/TRANSPONDER (MAT)

As mentioned previously, we recently had the opportunity to propose a combined Microlaser Altimeter Transponder (MAT) instrument on a NASA Discovery Mission to the asteroid Vesta. The intent was to map the surface reflectivity (at 532 nm) and topography (with decimeter accuracy) of the asteroid Vesta from orbit using single photon detection. In addition, during the interplanetary cruise phase and at selected times from Vesta orbit, the same instrument will demonstrate decimeter level ranging and subnanosecond time transfer from Earth to the spacecraft over a wide range of interplanetary distances (0.3 to 3.4 AU).
A block diagram of the dual altimeter/transponder has been previously provided in Figure 2. In altimeter mode, the incoming signal is the outgoing pulse reflected from the planetary or asteroid surface. In transponder mode, the incoming signal is a subnanosecond pulse originating from the Earth station.

The altimetry function introduces additional complications in the implementation of the correlation range receiver. First of all, the generating function for the surface return is not as highly peaked in range since it is broadened by the cumulative surface slope and roughness within the ground area illuminated by the laser during a frame, and this generally forces significantly wider range bins relative to ranging. Secondly, the altimeter „trajectory“ (in this case the height variability of the surface under investigation) is not highly predictable as it is in the ranging or transponder case, but we have demonstrated through computer simulation that somewhat analogous constraints on the „trajectory“ can nevertheless be applied based on a priori knowledge or estimates of nominal maximum surface slope and roughness [8,9]. Also, abrupt changes in „trajectory“ (e.g. a steep cliff) become possible, and the autotracking algorithms must be clever enough to recognize these sudden transitions between two widely displaced „valid trajectories“ by applying both forward-looking and backward-looking predictor/corrector techniques.

The dual instrument consists of the following major subsystems (see Figure 2):

> Transmitter optical assembly consisting of a space-qualified SLR2000 microlaser transmitter (260 mW, 2KHz, 532 nm), a 3 cm diameter transmit telescope, Risley prism point-ahead mechanism, and prism feedback into the receiver for transmitter pointing verification.
>
> Optical Receiver consisting of a 15 to 30 cm (depending on range) all-Beryllium telescope, a $\pm$ 0.5 degree FOV CCD camera for Earth/star/Moon sensing, a photon counting microchannel plate photomultiplier (MCP/PMT) with angle sensing capability (FOV ~ 90 arcseconds, angular resolution <1 arcsecond) , spectral and spatial filters, assorted interface optics, and two axis Image Motion Compensators (IMC’s) for fine pointing correction of the receiver.
>
> Electronics Box consisting of the real-time system controller, time and frequency reference (if not provided by the spacecraft), laser diode pump array, correlation range receiver (CRR), two dual-axis servo motor drivers for intermediate and fine correction of receiver/transmitter pointing (via IMC’s or steering mirror), and the thermal control system. An extremely lightweight, low power, single chip, all-digital version of the CRR can achieve range resolutions of several cm at few kHz rates. Higher resolution (few mm) is easily achieved with additional weight and prime power allocations but may not be justified if the range error is dominated by spacecraft attitude uncertainty in altimetry mode or by onboard clock stability in transponder mode.
>
> An optical bench mounted on a two axis tilt table for intermediate correction of the transmitter and receiver pointing or, if the instrument mass budget permits, a fixed optical bench with the laser transceiver looking though a limited range two-axis gimballed flat beryllium steering mirror (which can replace the tilt table and IMC’s). As described previously, Risley prisms in front of the small transmit telescope would provide differential pointing for the transmit beam.

10. CONCLUDING REMARKS

Since the feasibility of interplanetary microlaser transponders was first discussed at the last Workshop[1], significant progress has been made in defining a reasonably compact instrument capable of ranging anywhere within the inner Solar System. Our theoretical understanding of the technique and its underlying requirements have been enhanced, and viable methods for acquiring and tracking the opposite terminal have been developed. Successful field tests of the SLR2000 system, combined with our laboratory transponder tests, should remove most, if not all, of the technical uncertainty in proposing an interplanetary transponder mission over the next few years. In addition, we have recently been funded (as of December 1998) to develop and demonstrate, over a period of 32 months, a 10 kHz Airborne Microlaser Altimeter under NASA's Instrument Incubator Program. The combined technical and scientific results from these three programs should greatly enhance the credibility of dual purpose instrumentation like the Combined Microlaser Altimeter Transponder (MAT) and enhance its overall scientific value and desirability.

REFERENCES

1. Degnan, J. J., „Compact laser transponders for interplanetary ranging and time transfer", Proc. 10th International Workshop on Laser Ranging, pp. 24-31, Shanghai, China, November 11-15, 1996.

2. Degnan, J. J. and J. F. McGarry, „SLR2000: Eyesafe and autonomous single photoelectron satellite laser ranging at kilohertz rates", SPIE Proceedings Volume 3218, Laser Radar Ranging and Atmospheric Lidar Techniques, pp. 63-77, London, UK, September 24-27, 1997. (also see these proceedings)

3. Lemoine, F. J., NASA Goddard Space Flight Center, Greenbelt, MD 20771, USA, private communication.

4. McGarry, J.F., J. J. Degnan, P. Titterton, H. Sweeney, B. P. Conklin, and P. J. Dunn, „Automated tracking for advanced satellite laser ranging systems", Proc. Spring SPIE Meeting, SPIE Vol. 2739, pp. 89-103, Orlando, FL, April 10-11, 1996.

5. A. Mallama, Raytheon STX Corporation, Greenbelt, MD 20771 USA, private communication.

6. Degnan, J. J. , "Millimeter Accuracy Satellite Laser Ranging: A Review", Contributions of Space Geodynamics: Technology, D. E. Smith and D. L. Turcotte (Eds.), AGU Geodynamics Series, Volume 25, pp. 133-162, 1993.

7. Steggerda, C., C. B. Clarke, J. M. Heinick, D. McClure, M. Selden, R. Stringfellow, and G. Bianco, „Instrumentation development and calibration for the Matera Laser Ranging Observatory", Proc. 10th International Workshop on Laser Ranging, pp. 24-31, Shanghai, China, November 11-15, 1996.

8. Degnan, J.J., and J. F. McGarry, „Feasibility study of Multikilohertz Spaceborne Microlaser Altimeters", European Geophysical Society (EGS) Symposium, Nice, France, April 20-24, 1998, Annales Geophysicae, Part 1, Society Symposia, Solid Earth Geophysics and Geodesy, Supplement 1 to Volume 16, p. C379 (Abstract only).

9. Degnan, J. J. and J. F. McGarry, „Design and Simulated Performance of Compact Multikilohertz Microlaser Altimeters for Mapping Surface Topography from Space", 19th International Laser Radar Conference, Paper TBD, Annapolis, MD, July 6-10, 1998.